JOURNAL OF GEOPHYSICAL RESEARCH, VOL. 115, D10109, doi:10.1029/2009JD012961, 2010

Click Here for Full Article

Atmospheric warming at a high-elevation tropical site revealed by englacial temperatures at Illimani, Bolivia (6340 m above sea level, 16°S, 67°W)

A. Gilbert,[1,2] P. Wagnon,[2] C. Vincent,[3] P. Ginot,[1,2] and M. Funk[4]

Received 5 August 2009; revised 28 December 2009; accepted 4 January 2010; published 25 May 2010.

[1] In June 1999, a deep (138.7 m) ice core was extracted from the summit glacier of Illimani, Bolivia (6340 m above sea level, 16°39′S, 67°47′W), and an englacial temperature profile was measured in the borehole. Using on-site and regional meteorological data as well as ice core stratigraphy, past surface temperatures were reconstructed with a heat flow model. The englacial temperature measurements exhibit a profile that is far from a steady state, reflecting an increasing atmospheric temperature over several years and nonstationary climatic conditions. Englacial temperature interpretation, using air temperature data, borehole temperature inversion, and melting rate quantification based on ice core density, shows two warming phases from 1900 to 1960 (+0.5 ± 0.3 K starting approximately in 1920–1930) and from 1985 to 1999 (+0.6 ± 0.2 K), corresponding to a mean atmospheric temperature rise of 1.1 ± 0.2 K over the 20th century. According to various climate change scenarios, the future evolution of englacial temperatures was simulated to estimate when and under what conditions this high-elevation site on the Illimani summit glacier could become temperate in the future. Results show that this glacier might remain cold for more than 90 years in the case of a +2 K rise over the 21st century but could become temperate in the first 20 m depth between 2050 and 2060 if warming reaches +5 K.

Citation: Gilbert, A., P. Wagnon, C. Vincent, P. Ginot, and M. Funk (2010), Atmospheric warming at a high-elevation tropical site revealed by englacial temperatures at Illimani, Bolivia (6340 m above sea level, 16°S, 67°W), *J. Geophys. Res.*, *115*, D10109, doi:10.1029/2009JD012961.

1. Introduction

[2] Tropical glaciers are known to be very sensitive climatic indicators [e.g., *Francou et al.*, 2003, 2004; *Favier et al.*, 2004; *Vuille et al.*, 2008]. These high-altitude sites (usually above 4800 m above sea level (asl)) are particularly vulnerable to the effects of global warming [*Vuille et al.*, 2008]; however, direct meteorological observations are very scarce and generally discontinuous. Consequently, reconstructing air temperatures over recent decades or centuries using various proxies or modeling is particularly important at these locations.

[3] The temperature distribution within cold glaciers strongly depends on surface temperature variations and provides an excellent means to investigate past climate variations in polar regions [*Ritz*, 1989; *Salamatin et al.*, 1998] and on high mountains [e.g., *Haeberli and Funk*, 1991; *Lüthi and Funk*, 2001; *Vincent et al.*, 2007] with a time scale much larger for ice sheets than for high mountain areas. In the tropical Andes, cold glaciers are encountered usually above 6000 m asl and sometimes higher, depending on the site. Temperature measurements carried out during ice core drilling at 6270 m asl on Chimborazo (Ecuador) in November 2000 and at 6090 m asl on Nevado Coropuna (Peru) in June 2003 showed that the glaciers were temperate at these altitudes. The number of very high altitude cold glacier study sites in the tropics is therefore rather limited and likely to steadily decrease in the future because of global warming [*Thompson et al.*, 2006]. Nevertheless, borehole temperatures can provide very useful information on climate change at these high elevations where direct meteorological measurements are rare or sporadic [*Hardy et al.*, 2003; *Wagnon et al.*, 2003].

[4] For the Alps, *Lüthi and Funk* [2001] and *Vincent et al.* [2007] have concluded that borehole temperature profiles reflect conditions that are far from steady state and provide clear evidence of atmospheric global warming over recent decades. The profiles also reveal that the refreezing of surface meltwater below the surface contributes to the englacial temperature increase, even at elevations as high as 4250 m asl in the Alps [*Vincent et al.*, 2007]. In this study we present the first analysis of a vertical englacial temperature profile measured in the tropical Andes. It results from an ice core drilled on Illimani, Bolivia (6340 m asl, 16°39′S, 67°47′W).

[1]IHH, IRD, La Paz, Bolivia.
[2]LGGE and LTHE, IRD, Saint-Martin-d'Hères, France.
[3]LGGE, UJF, CNRS, Saint-Martin-d'Hères, France.
[4]VAW, ETH Zurich, Zurich, Switzerland.

Copyright 2010 by the American Geophysical Union.
0148-0227/10/2009JD012961



Figure 1. Location of the Illimani drilling site in South America.

In high-latitude ice caps, deep borehole temperature profiles are complementary to isotopic proxy to investigate past temperature fluctuations using inverse problem resolution [*Kotlyakov et al.*, 2004; *Nagornov et al.*, 2001; *Ritz*, 1989]. However, the Andean ice core isotopic signal is mostly associated with precipitation variations [*Vimeux et al.*, 2005, 2009] so that no reconstitution of temperature over recent centuries is yet available from Andean ice cores. After describing the data (section 2) and the model (section 3), we interpret borehole englacial temperature using La Paz air temperature (section 4) in order to reconstruct atmospheric temperature variations over the last century at 6340 m asl on Illimani (sections 5 and 6). In section 7 we assess the future evolution of englacial temperatures according to possible climate change scenarios. The conclusions are given in section 8.

2. Data

2.1. Site Location

[5] In June 1999, a 138.7 m ice core was drilled down to bedrock on a flat pass at 6340 m asl (16°39′S, 67°47′W), just below the main summit of Illimani (Cordillera Real, Bolivia) (Figure 1) [*Knüsel et al.*, 2003]. This site is located approximately 50 km southeast of the capital La Paz. The drilling site was chosen on the flattest location where the ice flow velocities are assumed to be very small. Results concerning chemical and isotopic analysis of this ice core are given by *De Angelis et al.* [2003] and *Ramirez et al.* [2003], respectively. Using volcanic signals in ice, *Knüsel et al.* [2003] have provided an accurate dating of this ice core with reference years located at 9.9 m (1991), 17.5 m (1982), 34.2 m (1963), and 64.4 m (1883). The total ice core covers approximately 18,000 years, and the upper 60 m cover the 20th century.

2.2. Measurements of Englacial Temperature and Density

[6] The boring was performed with a Fast Electromechanical Lightweight Ice Coring System (FELICS) [*Ginot et al.*, 2002]. The borehole always remained dry, thus limiting disturbance of the thermal regime. Drilling was completed on 3 June 1999 at 1240 LT. Englacial temperatures were measured using a 150 m long thermistor chain composed of 10 thermistors (Fenwal 135-103FAG-J01) located one every 5 m over the first 45 m of the chain. Each thermistor was previously calibrated in a thermostatic bath to reach ±0.05 K minimum accuracy. The chain was first installed in the borehole on 4 June 1999 at 1510 LT with the thermistors located between 138 and 93 m depth. Measurements were carried out with a digital multimeter (Fluke 83) used for calibration 1 h and 50 min later at 1700 LT and then also at

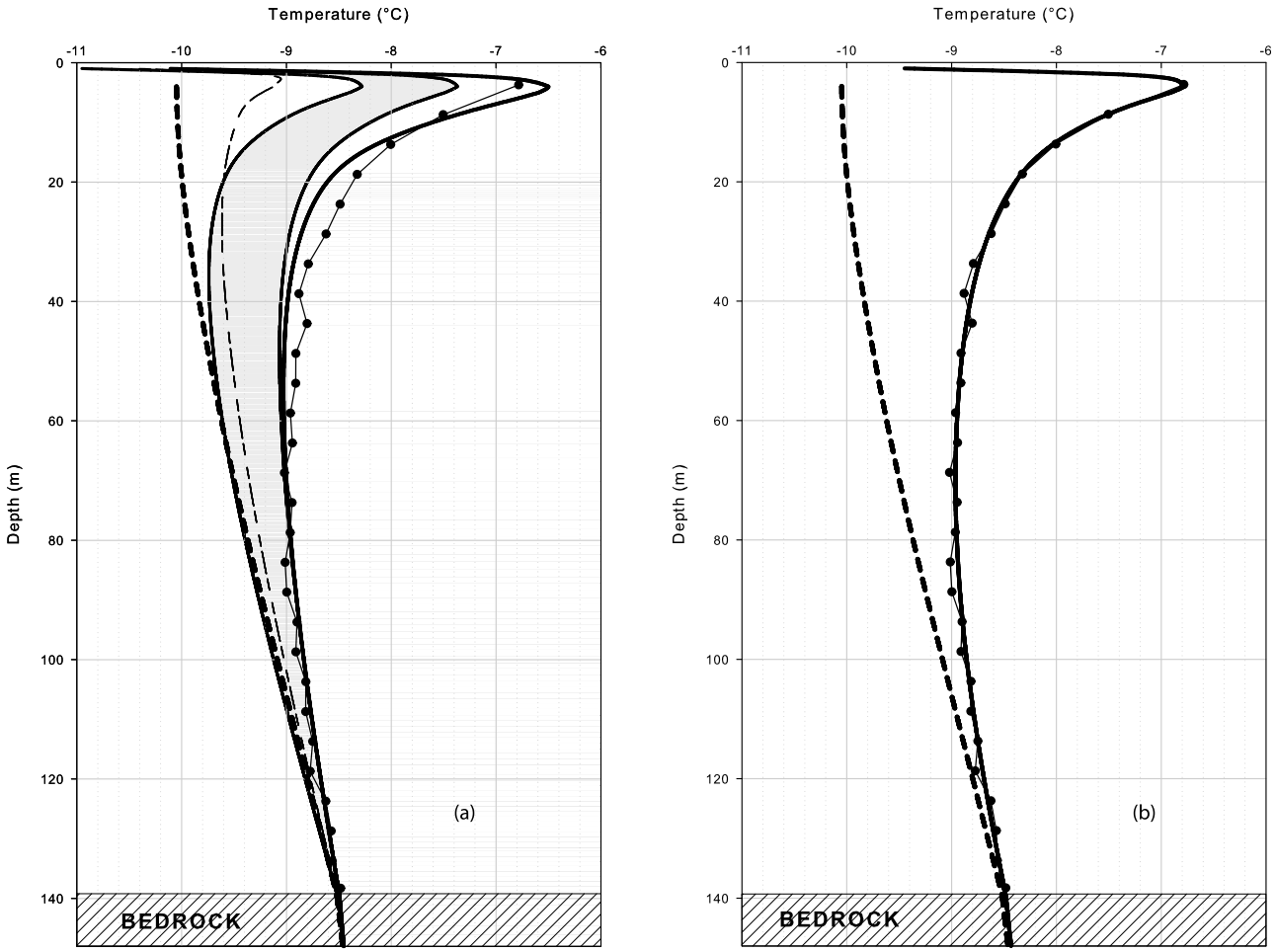


Figure 2. Vertical englacial temperature profile measured at Illimani (6340 m above sea level (asl)) in June 1999 (thin line with black dots). Modeled profile assuming a steady state climate with a constant secular temperature of 263.1 K (dashed line) and a constant geothermal flux of 22×10^{-3} W m^{-2}. (a) Modeled temperature profiles assuming a steady state before 1967 and using La Paz air temperature data after 1967 without taking into account the latent heat resulting from surface meltwater refreezing (thin dashed line) and taking into account the latent heat resulting from refreezing (melting factor a = 1.1 W m^{-2} K^{-1}) for a geothermal flux varying from 18 to 26×10^{-3} W m^{-2} (gray zone) and modeled temperature profile with a forced melting factor a = 1.7 W m^{-2} K^{-1} (thick line). (b) Modeled temperature profile assuming a steady state before 1900, assuming a 0.4 K warming between 1900 and 1962, and using La Paz air temperature after 1900 with a constant geothermal flux of 22×10^{-3} W m^{-2} and a melting factor of 1.1 W m^{-2} K^{-1} (thick line) (see section 4 for more details).

1730 and 1915 LT. Thirteen hours later, on 5 June, the chain was raised 50 m upward to perform measurements between 88 and 43 m at 0815 and 0930 LT. Finally, on 5 June, the chain was moved upward once again to measure the englacial temperatures between 38 m and the surface at 0930 and 1015 LT. The resulting englacial temperature profile with the resulting 28 points is plotted in Figure 2 (thin line with black dots).

[7] Density measurements were performed in cold rooms, measuring and weighing every section of the ice core ranging from 5 to 70 cm long, regardless of the time period covered by every section. Accuracy is assumed to be ±0.013 kg m^{-3}, taking into account the mass and size uncertainty of ice core sections. Ice layers were counted, and their thicknesses were measured along the core.

2.3. Meteorological Data Sets

[8] Since 1962, minimum and maximum daily air temperatures have been recorded in La Paz (El Alto meteorological station, 4070 m asl). Daily air temperature is approximated by the median value of the minimum and maximum values. Air temperatures were also measured (using Vaisala temperature thermistor with Gill Aspirated Radiation Shield (airflow monitoring switch)) at the drilling site by an automatic weather station (AWS) between May 1998 and March 1999, initially at 3.5 m above the surface. This data set was kindly provided by D. Hardy (University of Massachusetts).

[9] La Paz temperatures were compared with reanalyzed daily temperatures from NCEP-NCAR (15°S, 67.5°W, 500 hPa, since 1948, 2.5° grid) and with the AWS data set. La

Paz air temperatures show a difference between the mean temperature of the dry season and the mean temperature of the wet season as high as 4 K, which is similar to the seasonal thermal variability observed on Illimani by the AWS. On the other hand, reanalyzed temperatures do not agree well with AWS temperatures, particularly with a seasonal thermal variability not exceeding 2 K. Consequently, to simulate the heat flow into the glacier, La Paz temperatures seem to be more reliable than reanalyzed data.

3. Heat Flow Modeling

[10] The heat transfer equation within a cold glacier can be written as follows [*Malvern*, 1969; *Hutter*, 1983]:

$$\rho C_p \left[\frac{\partial T}{\partial t} + \mathbf{v} \cdot \mathbf{grad}(T)\right] = \mathrm{div}[k\ \mathbf{grad}(T)] + Q, \qquad (1)$$

where T (K) is the firn/ice temperature, ρ (kg m^{-3}) is the density, C_p (J kg^{-1} K^{-1}) is the thermal capacity, k (W m^{-1} K^{-1}) is the thermal conductivity, $\mathbf{v}$ (m s^{-1}) is the glacier flow velocity vector, t (s) is the time, and Q (W m^{-3}) is the latent heat released during water change of state per unit of time and volume. According to a similar study in the Alps [*Vincent et al.*, 2007], heat production by deformation and horizontal heat transfer can be neglected assuming that on this large flat pass, ice flow is slow and the horizontal englacial temperature gradient low. Consequently, equation (1) can be simplified to one dimension (z):

$$\rho C_p \left(\frac{\partial T}{\partial t} + v_z \frac{\partial T}{\partial z}\right) = \frac{\partial}{\partial z}\left(k \frac{\partial T}{\partial z}\right) + Q, \qquad (2)$$

where v_z (m s^{-1}) is the vertical glacier flow velocity.

[11] Englacial temperatures and their changes are computed at 10 day intervals using a Crank-Nicholson scheme (implicit finite difference) with a 1 m horizontal layer thickness. The geothermal flux is assumed to be constant at 10 m below the bedrock. *Noetzli et al.* [2007] showed that the three-dimensional topography has a strong influence on the heat flux variation in the summit areas of mountains, but we had no alternative other than to assume a constant geothermal flux. The temperature gradient inferred from the deepest 20 m above the bedrock allows us to assess the basal heat flux ($22 \pm 4 \times 10^{-3}$ W m^{-2}). According to the age-depth relationship, the vertical velocity is fitted by an exponential law ($v_z = v_0 \exp(-0.038z)$, $R^2 = 0.83$) with a surface vertical velocity v_0 given by the annual accumulation rate reconstructed by annual layer counting (mean value at Illimani is 0.58 m water equivalent) [*Knüsel et al.*, 2003]. The firn thermal conductivity k (W m^{-1} K^{-1}) is calculated using the Sturm density-conductivity relationship [*Sturm et al.*, 1997]

$$k = \begin{cases} 0.138 - 1.01\rho + 3.233\rho^2 & \text{if } 0.156 < \rho < 0.6 \\ 0.023 + 0.234\rho & \text{if } \rho < 0.156, \end{cases} \qquad (3)$$

where ρ is the firn/snow density. For densities higher than 0.6, we still apply equation (3) as suggested by *Sturm et al.* [1997].

[12] Surface boundary conditions depend on the surface energy balance. Modeling the surface energy budget requires meteorological data (incoming net all-wave radiation, albedo, air humidity, air and surface temperatures, and wind speed), which are usually not available on site [*Wagnon et al.*, 2003]. Consequently, the surface temperature T_{surf} (K), which is the snow temperature in the first meter of the glacier, is given by the simple parameterization [*Lüthi and Funk*, 2001]

$$T_{\mathrm{surf}} = T_{\mathrm{air}} - b, \qquad (4)$$

where T_{air} (K) is air temperature and b (K) is a parameter. At Illimani, air temperature is also not known. Thus, in section 4, b can be regarded as a tuning parameter rather than as a physical one because it results not only from the surface energy balance but also from the lapse rate used between La Paz and the drilling site and from the steady state temperature.

4. Results

4.1. Preliminary Results

[13] The first simulation was done assuming a steady state up to the year 1967, which means that the surface temperature is assumed to remain stable until this date. This secular temperature, which is the representative temperature of the steady state, has been tuned to fit the simulated temperature profile to measured basal temperature, resulting in a value of 263.1 K. Additionally, monthly means of La Paz air temperatures have been compared with monthly AWS air temperatures for the period May 1998 to March 1999 in order to calculate a mean lapse rate of −6.5 K km^{-1} (standard deviation of 0.4 K). Using this lapse rate, the mean annual air temperature of La Paz between 1962 and 1967 leads to a mean air temperature of 265.8 K at 6340 m asl for this period. Consequently, the parameter b of equation (4) is set to 2.7 K. The value of b clearly depends on the reference period used to represent the steady state. Nevertheless, because of the much lower warming recorded by La Paz air temperatures between 1962 and 1982, b does not vary much when longer reference periods are used. Indeed, b equals 2.70, 2.86, and 2.85 K when using 1962–1967, 1962–1977, and 1962–1982, respectively, as reference periods for the steady state.

[14] Using any b parameter mentioned in section 4.1 and La Paz temperatures, the simulation of englacial temperatures reveals strong differences with measurements carried out in 1999 (Figure 2a, thin dashed line). Indeed, the simulated englacial temperatures are too low. These differences are likely due to an additional energy contribution. We suggest that an additional energy flux could come from the latent heat due to refreezing of meltwater as previously observed on a high alpine site [*Suter et al.*, 2004].

4.2. Effect of Latent Heat Released by Refreezing Meltwater

[15] On this cold, high-altitude site (annual mean air temperature <267 K), it can be assumed that meltwater occasionally produced at the surface refreezes immediately below the surface, releasing an energy flux called $F_{\mathrm{refreezing}}$

(W m^{-2}). This energy flux can be assessed using the degree-day parameterization [e.g., *Hock*, 2003]

$$F_{refreezing} = \begin{cases} (T_{air} - T_{ref})a & \text{if } T_{air} > T_{ref} \\ 0 & \text{if } T_{air} \leq T_{ref} \end{cases} \quad (5)$$

where a (W m^{-2} K^{-1}) is a melting factor accounting for the energy flux produced by refreezing meltwater with respect to the latent heat of melting-freezing ($L_f = 3.34 \times 10^5$ J kg^{-1}). T_{ref} is a daily temperature threshold above which the daytime surface temperature may reach 273.15 K, thereby letting melting occur. Air temperature recorded on site by the AWS in 1998–1999 showed that when daily temperature is as high as 267.1 ± 0.2 K, part of the afternoon exhibits positive air temperatures and melting may occur. T_{ref} is then assumed to be 267.1 K. If we assume that meltwater refreezes immediately below the surface, melting occurring from time to time at the surface systematically produces a latent heat release in the surface layer, that is, in the first layer of our model. Within this first layer, mass is always conserved; only heat is gained in the case of refreezing meltwater. This assumption is supported by the fact that this high-altitude site remains cold, preventing melting from being strong enough to produce running water.

[16] Ice layers were observed in the core, and a mean value of 6.8% in volume is measured in the first 37 m of the core [*Knüsel et al.*, 2003]. Taking into account the density difference between ice (920 kg m^{-3}) and firn in the upper layers (350 kg m^{-3}), the mean amount of calculated refreezing meltwater (between 1960 (37 m deep) and 1999 (surface)) is converted into a mean amount of ice layers along the core between the surface and 37 m deep. The factor a is then tuned to obtain the best agreement between the calculated and measured volume of ice within the core. We found $a = 1.1 \pm 0.1$ W m^{-2} K^{-1}, corresponding to 0.48 ± 0.03 mm K^{-1} d^{-1} in a classical degree-day formulation. This low value compared with usual snow degree-day factors [*Hock*, 2003] can be explained by the fact that this very high altitude site is cold and characterized by a continually high albedo surface and strong sublimation rates [*Wagnon et al.*, 2003].

[17] In sections 5 and 6 we use equation (5) at annual time scale. The linear regression between annual mean air temperature and annual surface melting computed with the previous degree-day approach gives a good correlation (R^2 = 0.80, n = 37 years). Thus, annual melting and annual temperature are related by (5) with $T_{\mathrm{ref}} = 265.3 \pm 0.1$ K and a = 0.53 ± 0.03 W m^{-2} K^{-1}.

[18] Using this additional flux from heat released by the refreezing of surface meltwater and assuming a steady state up to 1967 improves agreement with measurements (Figure 2a). Nevertheless, simulated englacial temperature profiles between 10 and 60 m deep still remain colder than the observed profile, no matter what melting factor or geothermal flux values are used (the gray zone in Figure 2a shows simulated profiles for a basal heat flux varying between 18 and 26 × 10^{-3} W m^{-2} and the thick line shows a melting factor forced to 1.7 W m^{-2} K^{-1}). A nonstationary climatic state before 1967 could explain this remaining lack of energy. For this reason, the assumption relative to climatic steady state before 1967 was rejected.

[19] On the other hand, we can assume a climatic steady state until 1900. Indeed, from numerical experiments, it can be shown that temperature variations before 1900 do not influence the 1999 englacial temperature profile. As a matter of fact, the continuity between the steady climatic state before 1900 and La Paz air temperature data is interrupted if the parameter b (equation (4)) remains related to the secular temperature (as in section 4.1). Consequently, as for the geothermal flux and the secular temperature, b is used to adjust the simulated profile to the observed profile. Since simulated and observed englacial temperatures mainly differ in the upper 60 m (Figure 2a), these three parameters are strongly constrained by this part of the profile. The set of parameters providing the best agreement between observations and simulations gives a geothermal flux of 21 ± 2 × 10^{-3} W m^{-2}, a secular temperature of 263.1 ± 0.1 K, and b of 2.3 ± 0.1 K. Figure 2b shows the englacial temperature profile simulated with this set of parameters using La Paz air temperatures. According to equation (4) and considering the values obtained for the secular temperature and for b, air temperature before 1900 is assumed to be 265.4 ± 0.2 K while the mean La Paz air temperature between 1962 and 1967 is 265.8 K. This implies a 0.4 ± 0.2 K atmospheric warming between the steady state (before 1900) and the mean temperature over the 1962–1967 period.

[20] In conclusion, the observed englacial temperature profile of Illimani can be explained only if we take into account both the latent heat released by the refreezing of surface meltwater and a 0.4 ± 0.2 K atmospheric warming at 6340 m asl between the beginning of the 20th century and the 1960s. An accurate parameter sensitivity test is now needed to confirm and improve the temperature reconstitution over the 20th century at this high-altitude site. This test is performed in section 5 using inverse problem analysis.

5. Borehole Temperature Profile Inversion

5.1. Bayesian Approach to Solving the Inverse Problem

[21] Bayesian inference, described by *Hopcroft et al.* [2007], was applied to assess the past surface temperature variations from englacial temperatures. This analysis was done without using La Paz temperatures for the last 37 years. In a Bayesian formulation, model parameters are described by probability distributions. The aim of Bayesian inference is to quantify the posterior probability distribution, which characterizes all of the model parameters given prior information and the data available.

[22] The past surface temperature (from 1900 to 1999) is set up as a series of linear segments with the nodes of these segments being the model parameters T_{surf}, i.e., $T_{\mathrm{surf}} = (T_i, t_i; i = 1, 5)$, where T is temperature and t is time (t_1 and t_5 are fixed at 1900 and 1999, respectively). The other parameters are the melting factor and the geothermal flux. The secular temperature is given by the geothermal flux and the basal temperature, according to steady state conditions (see section 4.1). The latent energy flux released by the refreezing of meltwater is estimated by a linear relationship between

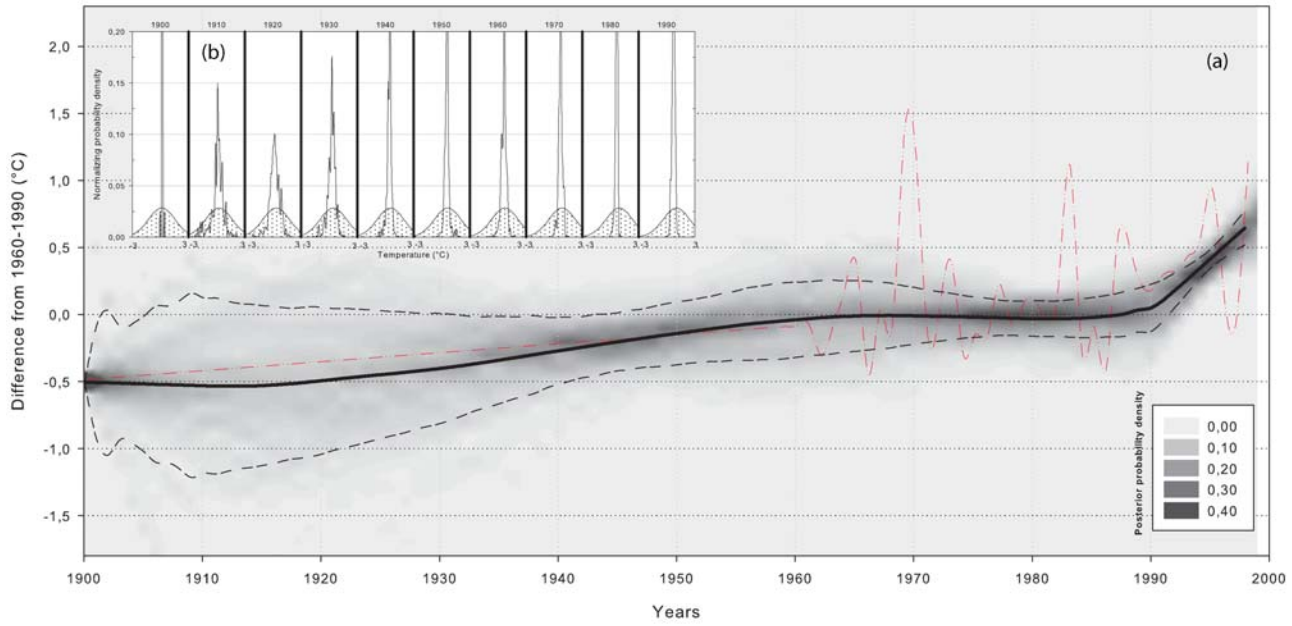


Figure 3. (a) Reconstructed air temperature at Illimani (6340 m asl) over the 20th century using borehole temperature profile inversion (thick line) compared with La Paz air temperature (red dashed line after 1962). The two black dashed lines form an envelope corresponding to model uncertainties according to posterior probability density standard deviation. The gray scale represents the past surface temperature probability distribution. (b) Posterior (thin line) and prior (dotted surface) probability density functions of surface temperature each 10 years (see section 5 for more details).

annual melting and annual temperature anomalies, according to equation (5) (see section 4.2).

[23] In order to determine posterior probability density function (pdf), the values of the parameters are generated according to the Markov Chain Monte Carlo method. The surface temperatures T_{surf}, the melting factor a, and the geothermal flux F_{geo} are updated for each iteration using a Gaussian random function.

[24] For each set of parameters, a posterior probability P is calculated using data and prior information according to

$$P = \exp\left[-0.5(\mathbf{T}_{model} - \mathbf{T}_{data})^T C^{-1}(\mathbf{T}_{model} - \mathbf{T}_{data})\right] \cdot \exp\left[-0.5(M_{data} - M_{model})^2 1/\sigma_M^2\right] \cdot P_{prior}(\boldsymbol{T}_{surf}) P_{prior}(a) P_{prior}(F_{geo}), \quad (6)$$

where $\mathbf{T}_{model}$ and $\mathbf{T}_{data}$ are the vectors of modeled englacial temperatures and measured englacial temperatures, respectively. C is the covariance matrix describing measurement uncertainty. The errors on the data are assumed to be uncorrelated, which implies C to be diagonal. M_{data} is the percentage of melting feature measured within the core (6.8%), while M_{model} is the same modeled percentage (see section 4.2); σ_M is the standard deviation, which specifies the measurement uncertainty on M_{data} (1%).

[25] The prior information, P_{prior}, used to constrain parameter values to realistic values is described by Gaussian probability functions. $P_{prior}(T_{surf})$ is centered on the surface temperature variations T_{prior}, which follows a linear trend of 0.01 K yr^{-1} over the period 1900–1999. The associated standard deviation is 1.5 K. $P_{prior}(a)$ is centered on the melting factor from section 4 (a_{prior} = 0.53 W m^{-2} K^{-1}), and the standard deviation is 0.5 W m^{-2} K^{-1}. $P_{prior}(F_{geo})$ is uniform over the interval [0, 0.080] W m^{-2}. Indeed, if the absolute difference between the parameters coming from Monte Carlo algorithm and prior parameters (T_{prior}, a_{prior}) exceeds one standard deviation, the associated posterior probability P tends toward zero.

[26] The resulting value of each parameter is the average of each value of this parameter obtained by the successive iterations and weighted by its probability. The model uncertainty is determined by the standard deviation of the posterior pdf.

5.2. Results

[27] In order to assess the accuracy of the model and to confirm the choice of the parameters used in section 4, a first sensitivity test was performed on the melting factor a and on the geothermal flux. We obtain a melting factor value of 0.5 ± 0.2 W m^{-2} K^{-1} on the annual time scale (close to the previous value estimated at 0.53 W m^{-2} K^{-1}, see section 4.2). Inversion does not give a better estimate of the geothermal flux than the use of the basal englacial temperature gradient (section 3). However, a fixed melting factor (0.5 W m^{-2} K^{-1}) gives a basal heat flux value of 21 ± 2 × 10^{-3} W m^{-2}, in agreement with the value obtained in section 4.2. The subsequent inversions will be performed using the melting factor and basal heat flux as fixed parameters equal to 0.5 W m^{-2} K^{-1} and 21 × 10^{-3} W m^{-2}, respectively (Figure 3).

[28] Using these fixed parameters and T_{surf} as a free parameter, our analysis was carried out to assess past temperature variations. According to the posterior pdf (Figure 3a, in gray scale), mean values of past temperature

Table 1. Twentieth Century Temperature Trends Reconstructed at Illimani[a]

	20th Century Warming (K)	Linear Temperature Trend (K decade^{-1}) (R^2)		
		1900–1999	1950–1999	1980–1999
Inversion with surface temperature as the free parameter	1.1 ± 0.2	0.085 ± 0.01 (0.88)	0.092 ± 0.02 (0.54)	0.35 ± 0.05 (0.81)
Reconstruction from density anomaly	1.2 ± 0.2	0.087 ± 0.02 (0.68)	0.13 ± 0.05 (0.50)	0.36 ± 0.1 (0.47)
Inversion with the surface temperature and geothermal flux as the free parameters	1.1 ± 0.3	0.10 ± 0.04 (0.79)	0.087 ± 0.03 (0.41)	0.42 ± 0.1 (0.88)
Inversion with the surface temperature, melting factor, and geothermal flux as the free parameters	1.0 ± 0.6	0.13 ± 0.05 (0.79)	0.066 ± 0.05 (0.16)	0.40 ± 0.15 (0.99)
Smoothed La Paz air temperature	-	-	-	0.28 ± 0.02 (0.90)
Southern Hemisphere global temperature trend [*Trenberth et al.*, 2007]	0.7 ± 0.2	[0.056,0.077][b]	-	[0.091,0.22][c]
Regional temperature trends from *Vuille et al.* [2003]. ECHAM-4 T106 altitude >6000 m asl	-	-	[0.05,0.10]	[0.30,0.40]

[a]Illimani, Bolivia (6340 m above sea level, 16°39′S, 67°47′W) with borehole temperature profile inversions, melting quantification, and La Paz air temperature compared with Southern Hemisphere global temperature trends [*Trenberth et al.*, 2007] and regional modeled temperature trends from *Vuille et al.* [2003].
[b]For 1899–2005.
[c]For 1979–2005.

variations are plotted and compared to La Paz air temperatures. The pdf standard deviation gives the model uncertainty. Figure 3b compares the posterior and prior pdf's for every decade. It can be seen that further back in time, the posterior distribution becomes progressively more influenced by the prior pdf. Note that the secular temperature before 1900 is given by the basal heat flux using the basal temperature gradient. Without this condition, the 1900 prior and posterior pdf's would be very similar, indicating that the englacial temperature profile cannot provide any information on atmospheric temperature before this date.

[29] This borehole temperature inversion shows two atmospheric warming phases of +0.5 ± 0.3 K from 1900 to 1960 (starting approximately in 1920) and +0.6 ± 0.2 K from 1985 to 1999, corresponding to a warming of +1.1 ± 0.2 K for the 20th century. The temperature trend at Illimani agrees fairly well with the results from *Vuille et al.* [2003] (see Table 1). Inversion with the geothermal flux as a free parameter gives a 20th century warming of 1.1 ± 0.3 K. Adding the melting factor as a free parameter gives a similar result but with a larger range of uncertainty (warming of 1.0 ± 0.6 K over the 20th century). Temperature trends are summarized in Table 1 for each reconstruction in comparison with global change for the Southern Hemisphere [*Trenberth et al.*, 2007] and model results from *Vuille et al.* [2003].

6. Temperature Reconstruction Using Firn Density Anomalies

[30] Surface meltwater refreezes just under the snow surface creating a density anomaly within the firn layer. This anomaly was quantified in every section of the ice core by comparing the measured density with a computed density obtained from an empirical firn densification model (Figure 4a) [*Herron and Langway*, 1980]. In each core section, this density anomaly corresponds to an excess mass due to an amount of refreezing meltwater. Using the age-

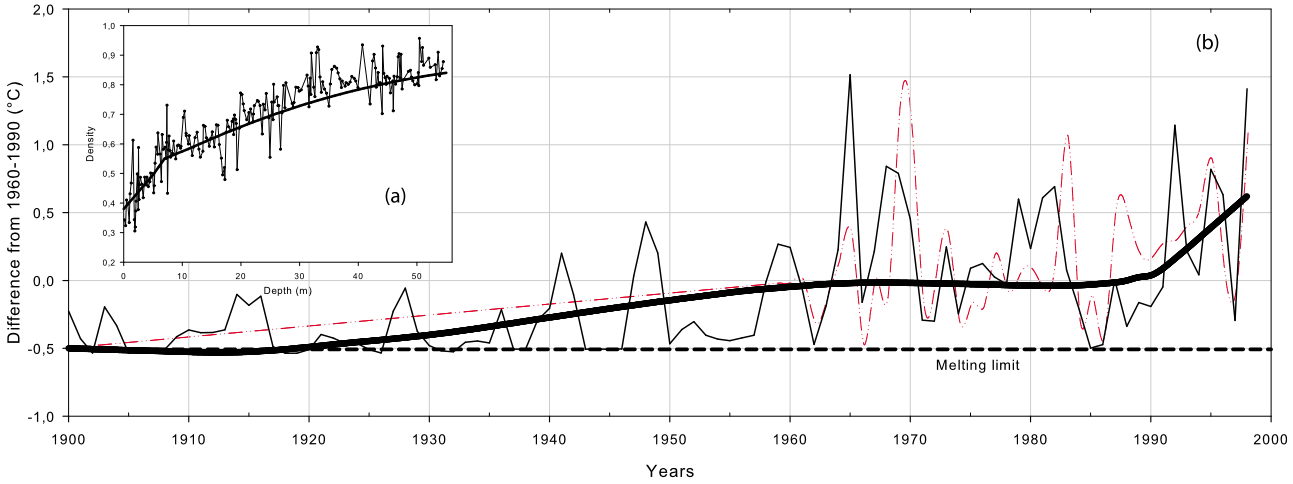


Figure 4. (a) Firn and ice density measured (thin line with black dots) and calculated according to *Herron and Langway*'s [1980] empirical firn densification model (thick line) in order to estimate density anomalies. (b) Density anomalies plotted as a function of the time in terms of temperature anomalies (thin line) (see section 6 for more details). These temperatures are compared with borehole temperature profile inversion (thick line) and La Paz air temperature (red dashed line after 1962).

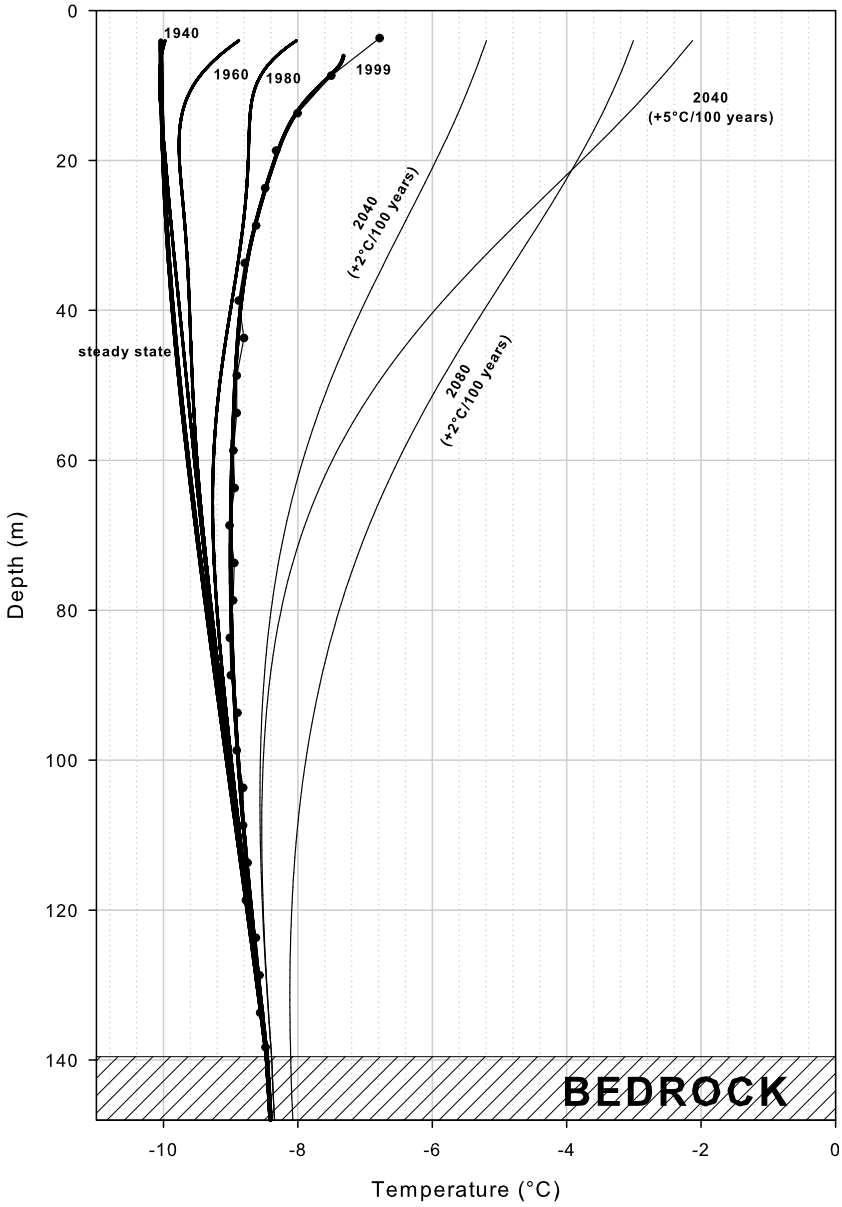


Figure 5. Simulated englacial temperature profiles in a borehole at Illimani (6340 m asl) over the 20th century (thick black lines), based on refreezing meltwater quantification with the density anomaly method compared with the observed June 1999 profile (thin line with black dots). Also shown are simulations over the 21st century (thin lines) according to two climate change scenarios (+2 K (100 years)$^{-1}$ and +5 K (100 years)$^{-1}$).

depth relationship given by *Knüsel et al.* [2003], the annual melting rate is reconstructed from 1900 to 1999. The latent heat corresponding to the annual amount of refreezing meltwater is then converted into annual air temperature according to the linear regression between air temperature and surface melting on the annual time scale used in section 4.2, a resulting from the inversion method ($a = 0.5$ W m^{-2} K^{-1}). The parameters of the densification model (surface temperature is 265.4 K, mean initial annual layer thickness is 0.58 m water equivalent yr^{-1}, and initial snow density is 380 kg m^{-3}) have been adjusted to obtain the best agreement between simulated (using the estimated annual amount of meltwater) and measured borehole englacial temperatures. These parameters are in good agreement with values reported by *Knüsel et al.* [2003], which gives confidence in the calibration. In the deepest part of the ice core (before 1940), the density measurement resolution was not accurate enough (some ice core sections covered more than a single year) to obtain a reliable annual melting quantification, making it necessary to use mean density values over several years. The resulting melting signal is therefore partly smoothed but does not influence the englacial temperature simulation.

[31] The resulting simulated 1999 profile fits the measured englacial temperature profile well (Figure 5). Temperature profile simulations for 1940, 1960, and 1980 are also plotted in Figure 5 and show that the glacier was near steady state until 1940 and then subject to strong warming

of englacial temperature, mainly due to the refreezing of surface meltwater.

[32] Reconstructing air temperature variations using melting quantification is a method which has been previously applied for alpine sites [*Henderson et al.*, 2006]. The comparison between the reconstructed temperature trends, using density anomalies or the inversion method and direct measurements from La Paz, shows good agreement (Figure 4b). For the method based on density anomalies, note that the absence of refrozen ice in an annual layer prevents us from inferring an annual temperature. It reveals that the annual temperature was lower than the reference temperature, i.e., 265.4 K. In this case, the annual temperature was set to this value.

7. Future Changes

[33] Using the same parameterization as in section 4.2, simulations for the future evolution of englacial temperature were computed according to possible future temperature change scenarios to assess when and under what conditions the high-altitude Illimani glacier could become temperate (Figure 5). Because of the strong effect of latent heat release by the melting-refreezing process, simulations show that englacial temperature may reach 273.15 K in the first 20 m depth between 2050 and 2060 with a warming of +5 K over the 21st century (estimated warming in the tropical Andes according to the SRES A2 emission scenario [*Vuille et al.*, 2008]). However, the glacier could remain cold with a reduced warming scenario of +2 K over the 21st century. These results need to be regarded with caution because simulations have been performed with the present tuned melting factor a, although because of changing energy balance factors, a is likely to change in the future.

8. Conclusion

[34] The borehole temperature profile measured in June 1999 at Illimani, Bolivia (6340 m asl, 16°39′S, 67°47′W) reflects conditions that are far from steady state. Indeed, the temperature distribution within this cold glacier provides clear evidence not only of atmospheric warming over the 20th century at this high-elevation site (1.1 ± 0.2 K over the period 1900–1999) but also of the effect of latent heat resulting from the refreezing of meltwater at the surface. Air temperature variations over the 20th century have been reconstructed using three different approaches. Two methods are based on a heat flow model: first, in a direct forward mode using a quantification of the surface melting with a degree-day approach using La Paz air temperature and, second, in an inverse mode to assess the sensitivity of each model parameter and to yield a confidence interval for air temperature trends. The third method, independent from the others, uses density anomalies along the ice core as quantification of melting-refreezing processes. The first method depends on La Paz air temperature and assumes that Illimani air temperature variations are similar to La Paz'. This assumption allows simulating borehole temperature, but there is no control on the melting factor. The second method provides a value of the melting factor and a surface temperature reconstitution independent from La Paz air temperature. The fact that both methods agree fairly well gives confidence in the results. The third approach to assessing temperature reconstitution at annual time scale yields similar temperature trends, which again strengthens the results. This high-altitude tropical site has exhibited accelerated atmospheric warming since 1985 with a 1900–1999 mean linear decadal temperature trend of 0.085 ± 0.01 K decade^{-1} and a 1980–1999 decadal trend of 0.35 ± 0.05 K decade^{-1}.

[35] At an annual time scale, Illimani and La Paz temperatures are not always in agreement as revealed by the density anomaly approach. Unfortunately, the resolution of Illimani ice core density measurements does not always allow a reliable surface melting reconstitution on an annual time scale. High-resolution density measurements would be required to improve the reconstruction and to yield reliable conclusions with this method.

[36] Temperature profile interpretation is also valuable to investigate future englacial temperature evolution according to various climate change scenarios. In the event of a +2 K rise over the 21st century, Illimani glacier at 6340 m asl is likely to remain cold, although with a +5 K warming, the glacier could reach 273.15 K in the first 20 m depth between 2050 and 2060, making ice core studies much less valuable for paleoclimatic investigations.

[37] Finally, in order to better constrain model parameters, it would be very useful to repeat englacial temperature measurements every 10 or 15 years at the same site, as in the Alps [*Vincent et al.*, 2007]. This is especially important nowadays at a time when atmospheric warming at very high elevations in the tropics appears to be accelerating.

[38] **Acknowledgments.** This study and the ice core drilling were funded by IRD (France) and PSI/University of Bern (Switzerland). We thank B. Zweifel for providing borehole temperature data and thermistor chain calibration, D. Hardy for AWS data, J.-D. Taupin and H. Bonnaveira for ice core density measurements, and the Bolivian, French, and Swiss institutions drilling teams. The thermistor chain has been kindly calibrated at ETH (Zürich, Switzerland). We thank three anonymous reviewers for their thorough reviews which efficiently helped to improve the manuscript.

References

De Angelis, M., J. Simões, H. Bonnaveira, J.-D. Taupin, and R. J. Delmas (2003), Volcanic eruptions recorded in the Illimani ice core (Bolivia): 1918–1998 and Tambora periods, *Atmos. Chem. Phys. Discuss.*, *3*, 2427–2463.

Favier, V., P. Wagnon, and P. Ribstein (2004), Glaciers of the outer and inner tropics: A different behaviour but a common response to climatic forcing, *Geophys. Res. Lett.*, *31*, L16403, doi:10.1029/2004GL020654.

Francou, B., M. Vuille, P. Wagnon, J. Mendoza, and J. Sicart (2003), Tropical climate change recorded by a glacier in the central Andes during the last decades, of the 20th century: Chacaltaya, Bolivia, 16°S, *J. Geophys. Res.*, *108*(D5), 4154, doi:10.1029/2002JD002959.

Francou, B., M. Vuille, V. Favier, and B. Cáceres (2004), New evidence for an ENSO impact on low-latitude glaciers: Antizana 15, Andes of Ecuador, 0°28′S, *J. Geophys. Res.*, *109*, D18106, doi:10.1029/2003JD004484.

Ginot, P., F. Stampi, D. Stampi, M. Schwikowski, and H. Gaggeler (2002), FELICS, a new ice core drilling system for high-altitude glaciers, *Mem. Natl. Inst. Polar Res.*, *56*, Spec. Issue, 38–48.

Haeberli, W., and M. Funk (1991), Borehole temperatures at the Colle Gnifetti core drilling site (Monte Rosa, Swiss Alps), *J. Glaciol.*, *37*, 37–46.

Hardy, D. R., M. Vuille, and R. S. Bradley (2003), Variability of snow accumulation and isotopic composition on Nevado Sajama, Bolivia, *J. Geophys. Res.*, *108*(D22), 4693, doi:10.1029/2003JD003623.

Henderson, K., A. Laube, H. W. Gäggeler, S. Olivier, T. Papina, and M. Schwikowski (2006), Temporal variations of accumulation and temperature during the past two centuries from Belukha ice core, Siberian Altai, *J. Geophys. Res.*, *111*, D03104, doi:10.1029/2005JD005819.

Herron, M., and C. Langway Jr. (1980), Firn densification: An empirical model, *J. Glaciol.*, *25*, 373–385.

Hock, R. (2003), Temperature index melt modelling in mountain areas, *J. Hydrol.*, *282*(1–4), 104–115, doi:10.1016/S0022-1694(03)00257-9.

Hopcroft, P. O., K. Gallagher, and C. C. Pain (2007), Inference of past climate from borehole temperature data using Bayesian reversible jump Markov Chain Monte Carlo, *Geophys. J. Int.*, *171*, 1430–1439, doi:10.1111/j.1365-246X.2007.03596.x.

Hutter, K. (1983), *Theoretical Glaciology: Material Science of Ice and the Mechanics of Glaciers and Ice Sheets*, D. Reidel, Dordrecht, Netherlands.

Knüsel, S., P. Ginot, U. Schotterer, M. Schwikowski, H. W. Gaggeler, B. Francou, J. R. Petit, J. C. Simoes, and J. D. Taupin (2003), Dating of two nearby ice cores from the Illimani, Bolivia, *J. Geophys. Res.*, *108*(D6), 4181, doi:10.1029/2001JD002028.

Kotlyakov, V. M., S. M. Arkhipov, K. A. Henderson, and O. V. Nagornov (2004), Deep drilling of glaciers in Eurasian Arctic as a source of paleoclimatic records, *Quat. Sci. Rev.*, *23*(11–13), 1371–1390, doi:10.1016/j.quascirev.2003.12.013.

Lüthi, M. P., and M. Funk (2001), Modelling heat flow in a cold, high-altitude glacier: Interpretation of measurements from Colle Gnifetti, Swiss Alps, *J. Glaciol.*, *47*(157), 314–323, doi:10.3189/172756501781832223.

Malvern, L. E. (1969), *Introduction to the Mechanics of Continuous Medium*, Prentice Hall, Englewood Cliffs, N. J.

Nagornov, O., Y. Konovalov, V. Zagorodnov, and L. Thompson (2001), Reconstruction of the surface temperature of Arctic glaciers from the data of temperature measurements in wells, *J. Eng. Phys. Thermophys.*, *74*(2), 253–261, doi:10.1023/A:1016661616282.

Noetzli, J., S. Gruber, T. Kohl, N. Salzmann, and W. Haeberli (2007), Three-dimensional distribution and evolution of permafrost temperatures in idealized high-mountain topography, *J. Geophys. Res.*, *112*, F02S13, doi:10.1029/2006JF000545.

Ramirez, E., et al. (2003), A new Andean deep ice core from Nevado Illimani (6350 m), Bolivia, *Earth Planet. Sci. Lett.*, *212*, 337–350, doi:10.1016/S0012-821X(03)00240-1.

Ritz, C. (1989), Interpretation of the temperature profile measured at Vostok, East Antarctica, *Ann. Glaciol.*, *12*, 138–144.

Salamatin, A. N., V. Y. Lipenkov, N. I. Barkov, J. Jouzel, J. R. Petit, and D. Raynaud (1998), Ice core age dating and paleothermometer calibration on the basis of isotope and temperature profiles from deep boreholes at Vostok Station (East Antarctica), *J. Geophys. Res.*, *103*(D8), 8963–8977, doi:10.1029/97JD02253.

Sturm, M., J. Holmgren, M. Konig, and K. Morris (1997), The thermal conductivity of snow, *J. Glaciol.*, *143*, 26–41.

Suter, S., M. Hoelzle, and A. Ohmura (2004), Energy balance at a cold, alpine firn saddle, Seserjoch, Monte Rosa, *Int. J. Climatol.*, *24*(11), 1423–1442, doi:10.1002/joc.1079.

Thompson, L. G., E. Mosley-Thompson, H. H. Brecher, M. E. Davis, B. Leon, D. Les, L. Ping-Nan, T. A. Mashiotta, and K. R. Mountain (2006), Abrupt tropical climate change: Past and present, *Proc. Natl. Acad. Sci. U. S. A.*, *103*, 10,536–10,543, doi:10.1073/pnas.0603900103.

Trenberth, K., et al. (2007), Observations: Surface and atmospheric climate change, in *Climate Change 2007: The Physical Science Basis. Contribution of Working Group I to the Fourth Assessment Report of the Intergovernmental Panel on Climate Change*, edited by S. Solomon et al., pp. 235–336, Cambridge Univ. Press, Cambridge, U. K.

Vimeux, F., R. Gallaire, S. Bony, G. Hoffmann, and J. C. H. Chiang (2005), What are the climate controls on δD in precipitation in the Zongo Valley (Bolivia)? Implications for the Illimani ice core interpretation, *Earth Planet. Sci. Lett.*, *240*, 205–220, doi:10.1016/j.epsl.2005.09.031.

Vimeux, F., P. Ginot, M. Schwikowski, M. Vuille, G. Hoffmann, L. G. Thompson, and U. Schotterer (2009), Climate variability during the last 1000 years inferred from Andean ice cores: A review of methodology and recent results, *Palaeogeogr. Palaeoclimatol. Palaeoecol.*, *281*, 229–241, doi:10.1016/j.palaeo.2008.03.054.

Vincent, C., E. Le Meur, D. Six, P. Possenti, E. Lefebvre, and M. Funk (2007), Climate warming revealed by englacial temperatures at Col du Dôme (4250 m, Mont Blanc area), *Geophys. Res. Lett.*, *34*, L16502, doi:10.1029/2007GL029933.

Vuille, M., R. S. Bradley, M. Werner, and F. Keimig (2003), 20th century climate change in tropical Andes: Observations and model results, *Clim. Change*, *59*, 75–99, doi:10.1023/A:1024406427519.

Vuille, M., B. Francou, P. Wagnon, I. Juen, G. Kaser, B. Mark, and R. Bradley (2008), Climate change and tropical Andean glaciers: Past, present and future, *Earth Sci. Rev.*, *89*, 79–96, doi:10.1016/j.earscirev.2008.04.002.

Wagnon, P., J.-E. Sicart, E. Berthier, and J.-P. Chazarin (2003), Wintertime high-altitude surface energy balance of a Bolivian glacier, Illimani, 6340 m above sea level, *J. Geophys. Res.*, *108*(D6), 4177, doi:10.1029/2002JD002088.

M. Funk, VAW, ETH Zurich, Rämistrasse 101, CH-8092 Zürich, Switzerland.

A. Gilbert, P. Ginot, and P. Wagnon, LGGE, IRD, BP 96, F-38402 Saint-Martin-d'Hères CEDEX, France. (latsfouine@hotmail.com)

C. Vincent, LGGE, UJF, CNRS, BP 96, F-38402 Saint-Martin-d'Hères CEDEX, France.